MERITS OF FLAPPING ROLL STABILIZER FINS

R.P.Dallinga, MARIN, The Netherlands
S.Rapuc, MARIN, The Netherlands

1. SUMMARY

Since their introduction in the late 1990s, the use of fin stabilizers in the stabilization of rolling ships at zero forward speed has become quite common. This stabilization is generally achieved with more or less conventional low-aspect ratio fins with increased actuator power to realize a "kicking" motion. The limitations of this compromise and a wealth of literature on "flapping flight" led MARIN in 2008 to explore the merits of a flapping fin alternative by means of a set of experiments. The present work describes, after a general introduction, the results of these tests and a comparison with the conventional solution. In addition the results of very recent experiments with a commercial application of the principle are discussed.

2. INTRODUCTION

In the late 1990's MARIN suggested using low-aspect ratio stabilizer fins in a "kicking" mode to stabilize the roll of a motor yacht at zero speed. After publication [Dallinga, 1999], the industry quickly recognized the potential and developed a range of products that make use of the principle; nowadays stabilizers with a "zero-speed" mode are quite common for this kind of ship.

To obtain reaction forces at zero speed the normal "zero-speed" fin is a more or less conventional stabilizer fin with a low aspect ratio and an eccentric shaft position. This geometry is a compromise with the optimum arrangement for transit conditions.

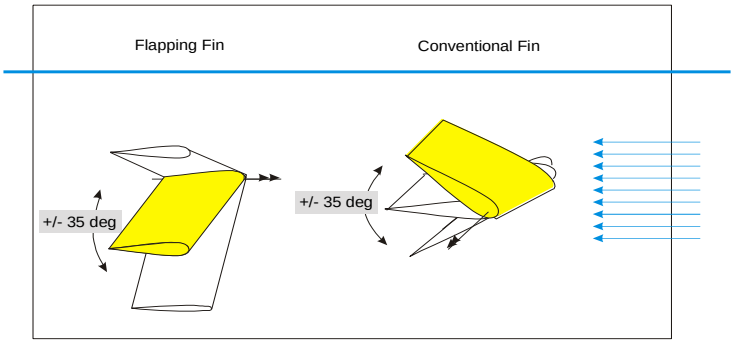

Figure 1 [*Fin Operating Modes*]

One point concerns the performance of a low aspect ratio fin in transit. The related low lift-slope leads to relatively large fin angles which in turn yield a relatively large root-gap, resulting in relatively low stabilizing performance and a relatively high drag. In addition the position of the fins in the bilge leads to considerable interaction with the bilge keels ahead of and behind the fins, interactions which downgrade the overall performance.

Another point is the efficiency of the kicking motion that is used at zero speed in generating a transverse force, limitations in the eccentricity of the fin shaft imply that only the aft part of the fin contributes to the desired reaction force.

Last but not least, the "solution" for these issues, a relatively large fin, yields a drag penalty in transit.

The above observations and developments in research on flapping flight [Licht, 2004, Soueid, 2005] led MARIN to investigate the merits of a high-aspect ratio "flapping" fin rotating along an axis parallel to the centre line of the ship. This investigation was conducted in 2008.

Figure 2 [*AntiRoll fin design*]

Although the interpretation of these exploratory measurements was hampered by limitations of digital servo engines of the day, the results were sufficient to inspire AntiRoll BV to develop a practical application of the principle. This system consists of a retractable high aspect ratio fin with a dual rotating mechanism. This innovation allows switching of the operation between a conventional rotation mode and a flapping mode. The hydrodynamic performance of the concept was the subject of a theoretical study in 2013 and detailed model testing in the spring of 2014.

3. FIN REACTION FORCES, CONTROL AND ROLL DAMPING

3.1 Fin reaction forces

3.1 (a) Zero speed

As will be demonstrated, the forces at zero speed can be estimated to some extent by regarding them as the sum of an inertia and a drag component. The inertia component is the product of the "added mass" and the acceleration of the fin. The drag follows from the exposed area and the square of the fin velocity. Because the mechanical velocity and acceleration of the fin are relatively high, the roll and wave induced hydrodynamic water velocities and accelerations as well as memory in the generated flow can be neglected.

A practical implementation of the above principle evaluates the forces in a "strip"-wise manner, neglecting the interactions between the individual strips. For the conventional rotation mode, the integration is chord-wise; the estimate of the added mass assumes the proximity of the ship side shell. For the flapping mode the integration is span-wise.

3.1 (b) Transit

Work in the MARIN Cooperative Research Ships (CRS) addressed the reaction forces of conventional high- and low-aspect ratio fin stabilizers in transit. The developed calculation method recognizes that the basic lift-drag characteristics, which are determined by the planform, aspect ratio, thickness and area (see Hoerner, 1965, van Oossanen, 1981), require a correction for the fact that the fin is operating on a curved surface, below a free surface and in the boundary layer of the ship.

In the above method a panel code is used in the evaluation of the actual angles of attack; the method accounts for the motion and wave induced local cross-flow velocities along the bilge. In this way the contribution of the fin stabilizers to the roll excitation (through the wave induced false angles of attack) is accounted for.

Last but not least, the calculated fin forces require a correction for a substantial frequency-dependent fin-to-hull interaction (see Dallinga, 1993).

The reaction forces of "flapping" fins at increasing forward speed change from inertia and drag driven forces at low speed to lift dominated reaction forces at high speed. The evaluation of the forces is complicated because the angles of attack at modest forward speed are extremely large. The physics resembles that of "dynamic stall" (Gaillarde, G., 2003), a problem that complicates the definition of exact operational limits for conventional stabilizer fins.

3.2 Fin control

3.2 (a) Zero speed

As will be shown in the next section, a simple way to increase the effectivity of zero-speed operation is to generate a high reaction force at the moment the roll velocity is highest. This can be achieved with a "bang-bang" mode in which the fin is moving fast from one extreme position to the other. In this case the fin motion trajectory may be regarded as a sequence of an acceleration, a constant-speed transit and a deceleration.

A first objective of a zero-speed control strategy consists of maximizing the overall work of the reaction force in roll within the constraints of the actuator (torque, velocity). A second objective is to avoid exposing passengers to the unpleasant jerk associated with transient forces. Last but not least, it may be very economic to reduce fin activity if the roll amplitudes hardly contribute to passenger discomfort.

3.2 (b) Transit

In transit stabilizer fins are often operated in a passive mode if the comfort requirements are met. In higher waves the fins become active with a mechanical reaction on the roll and roll velocity. The first reaction limits any low-frequency response of the ship due to, for instance, wind gusting and steering and wave induced excitation at low encounter frequencies. The reaction on the roll velocity suppresses the resonant roll response due to excitation at the natural frequency of roll.

Experience from model tests shows that a simple PD control yields a very satisfactory roll reduction. A common way to estimate the control gain is by assuming that the fins should work at their "limits" when the criterion of roll is reached. The limits can refer to the maximum mechanical angles or the effective angles of attack in relation to (an assumption on) stall.

In principle there is a wide range of secondary objectives which could be addressed. One can think of reducing the drag by avoiding "unnecessary" large fin reactions (if the roll angles are below a particular criterion), avoiding the wave induced roll excitation originating in the wave induced false angles of attack on the fins with a force feedback and avoiding the perils of loss of lift due to stall. For conventional and flapping fins alike, one can speculate on a control strategy which maximizes the forward thrust due to the wave and motion induced false angles of attack.

3.3 Roll damping

The key factor relating the fin reaction forces to the equivalent linear damping b_{EL} is the dissipated power P of the fin reaction moment M_x counteracting the roll velocity $\dot{\varphi}$. It is given by:

$$b_{EL} = \frac{P}{\sigma_{\dot{\varphi}}^2} \text{ in which } P = \frac{\int_0^T M_x.\dot{\varphi}.dt}{T}$$

If the reaction moment M_x is proportional to the roll velocity (as in the case of the wave making damping), the dissipated power is proportional to the rms roll velocity $\sigma_{\dot{\varphi}}$ squared. This means that the roll damping is independent of the roll amplitude.

In the case where quadratic drag forces dominate the reaction forces (as for the drag from bilge keels), the work increases with the third power of the roll amplitude. In this case the equivalent linearized damping is proportional to the roll amplitude.

Because in the case of zero-speed operation the reaction forces are governed by the inertia and drag forces induced by local, relatively high velocities and accelerations of the fin, the reaction forces are virtually independent of the roll velocity. Consequently the work in roll is proportional to the roll amplitude and the equivalent linearized damping declines with the roll amplitude. This characteristic is also partly observed in case of stabilization by means of anti-roll tanks [Dallinga, 2002].

Because the lift slope of conventional stabilizer fins is quite linear, the reaction forces of passive fins at forward speed are proportional to the roll velocity as long as the angles of attack stay below the stall angle. If the mechanical reaction of the fin is also proportional to the roll velocity, the reaction forces due to the fin activity behave in the same way. In this case the effective damping is independent of the roll amplitude.

Once the fins start reaching their mechanical limits or if the (sum of the false and mechanical) angles of attack reach (the poorly defined) stall angle the effective linearized damping will reduce with increasing roll amplitude.

4. SIMPLE ESTIMATES OF ZERO-SPEED REACTION FORCES AND DAMPING FROM FLAPPING FINS

4.1 Fin reaction forces from a strip-wise analysis

4.1 (a) Flapping fin

Assuming a fin with span s and chord c, rotating around the base and neglecting end-effects the added mass $a_{\alpha\alpha}$ can be estimated from the 2D sectional added mass a′. Neglecting free-surface effects the 2D value equals $\rho.\pi.(c/2)^2$. The reaction force and the moment around the base become:

$M_{xI} = \int_0^s \ddot{\alpha}\,.x.a'.x.dx = \ddot{\alpha}\frac{1}{3}a's^3 = \ddot{\alpha}\frac{1}{12}\rho\pi c^2 s^3$ and $F_{yI} = \int_0^c \ddot{\alpha}\,.x.a'.dx = \ddot{\alpha}\frac{1}{2}a's^2 = \ddot{\alpha}\,\frac{1}{8}\rho\pi c^2 s^2$

The ratio of the moment and the reaction force (the arm of the reaction force) becomes two-thirds of the span s.

Assuming a quadratic local drag force, proportional to the chord, the moment and reaction force become:

$M_{xD} = \int_0^s c_D\frac{1}{2}\rho(\dot{\alpha}.x)^2.c.x.dx = \dot{\alpha}^2\frac{1}{8}\rho c_D.c.s^4$ and $F_{yD} = \int_0^s c_D\frac{1}{2}\rho.(\dot{\alpha}.x)^2.c.dx = \dot{\alpha}^2.\frac{1}{6}\rho c_D.c.s^3$

The arm of the drag component in the reaction force is three-quarters of the span.

4.1 (b) Conventional fin

If the fin were mounted on a flat base plate, the expected sectional added mass increases to $\rho.\pi.s^2/2$. Reversing the chord and span and assuming a shaft position at a distance a from the "leading" edge the inertia components become:

$M_{xI} = \int_{-a}^{c-a} \ddot{\alpha}\,.x.a'.x.dx = \ddot{\alpha}\frac{1}{6}\rho\pi s^2[(c-a)^3 + a^3]$ and $F_{yI} = \int_{-a}^{c-a} \ddot{\alpha}\,.x.a'.dx = \ddot{\alpha}\frac{1}{4}\rho\pi s^2[(c-a)^2 - a^2]$

The moment and force from the drag force become:

$M_{xD} = \int_{-a}^{c-a} c_D \frac{1}{2}\rho(\dot{\alpha}.x)^2.s.x.dx = \dot{\alpha}^2 \frac{1}{8}\rho c_D.s.[(c-a)^4 - a^4]$ and

$F_{yD} = \int_{-a}^{c-a} c_D \frac{1}{2}\rho(\dot{\alpha}.x)^2 s.dx = \dot{\alpha}^2 \frac{1}{6}\rho c_D s[(c-a)^3 + a^3]$

4.2 Work in roll and roll damping from a harmonic fin motion

If we assume a flapping fin going through a sinusoidal motion $\alpha_a.\sin(\omega.t + \varepsilon)$ with amplitude α_a with the same frequency ω as the roll motion $\varphi_a.\sin(\omega.t)$ (see Figure 3) the mean power dissipated by the reaction force F of a single fin performed in roll becomes:

$$P_F = \frac{\int_0^T \omega.\varphi_a \cos(\omega t).(-\omega^2\alpha_a \sin(\omega t+\varepsilon)\frac{1}{8}\rho\pi c^2 s^2 + \omega\alpha_a \cos(\omega t+\varepsilon).|\omega\alpha_a \cos(\omega t+\varepsilon)|.\frac{1}{6}\rho c_D c s^3)}{T}$$

$$= \omega.\varphi_a.(\omega^2.\alpha_a \frac{1}{16}\rho.\pi.c^2.s^2.sin(\varepsilon) - \omega^2\alpha_a^2.\frac{4}{18\pi}\rho.c_D.c.s^3.cos(\varepsilon))$$

In the above ε denotes the phase lead of the fin angle with respect to the roll motion. The optimum value of the phasing of fin motion depends on the contribution of the drag.

The damping follows from the mean power of the moment of the above force around the ship CoG and the orientation of the fin with respect to the arm to the CoG. Assuming 2 fins with an arm r and assuming a mean fin orientation along the arm to the CoG the roll damping becomes:

$$b_\varphi = \frac{2.P_F.r}{\frac{1}{2}.(\omega.\varphi_a)^2}$$

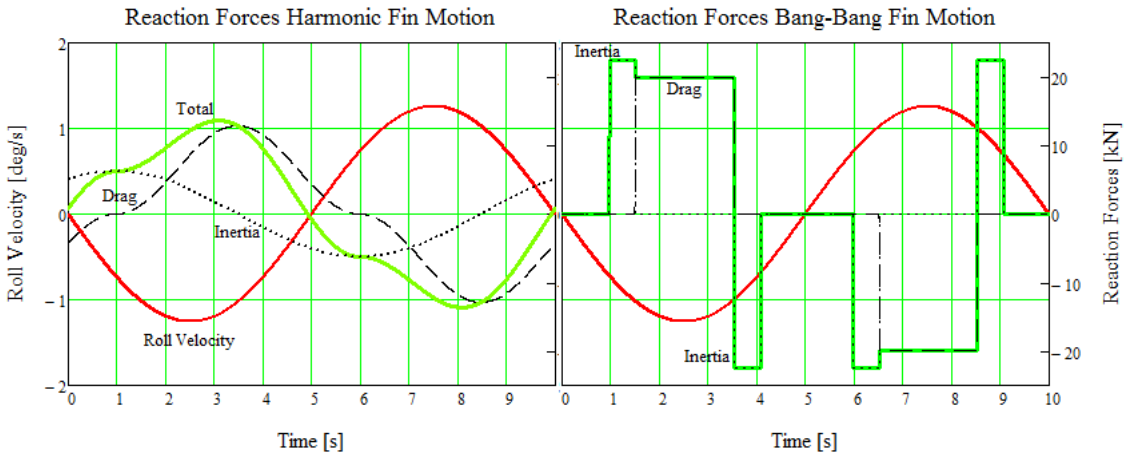

Figure 3 [*Reaction forces from a harmonic and a bang-bang fin motion*]

4.3 Work in roll and roll damping from a bang-bang fin motion

Because the roll period of many ships is fairly long and because the angular range of the fins is limited, the acceleration and velocity and related inertia and drag forces become relatively small. In this case, concentrating higher reaction forces around the maximum roll velocity is a way to enhance the damping.

As a practical case, we considered the application of a constant torque over the initial acceleration and the constant-velocity transit stage. In this case, the initial acceleration follows roughly from the added inertia and the transit-velocity from the drag moment per unit angular velocity squared. Neglecting the increasing velocity, the duration of the initial acceleration is simply

the ratio of transit velocity and the acceleration; the duration of the transit stage follows from the fin angle range and the velocity.

If we assume active deceleration (by means of the actuator) its magnitude equals that of the acceleration, in which case the contributions to the impulse cancel each other if they occur more or less symmetrically with respect to the peak in the roll velocity. In this case the magnitude of the work tends towards the product of the drag force, roll velocity and the duration of the constant-speed transit stage with increasing available constant actuator moment M*. In this case the reaction force F_{yDc}, the dissipated power P_{Fc} and roll damping $b_{\phi c}$ simply become:

$$F_{yDc} = \frac{8}{6}.\frac{M^*}{s} \text{ so } P_{Fc} = \omega.\varphi_a.F_{yc} = \omega.\varphi_a\frac{8}{6}.\frac{M^*}{s} \text{ and } b_{\varphi c} = \frac{16}{3}.\frac{M^*}{s.\omega.\varphi_a}$$

To illustrate the effect of available actuator torque and the difference between a harmonic and a shorter transient motion the work sample calculations were made for a fin with span s=4m, chord c=2m moving over a 2x35deg range. The assumed drag coefficient was c_D=4; the sample roll amplitude and period were 2deg and 10s. Figure 4 below compares the dissipated power in roll of a single fin from a sinusoidal and a constant-moment approach. It is clear that the harmonic fin motion is relatively ineffective. The combined effect of the higher reaction force and a shorter duration of the constant-velocity stage yields a dissipated power in roll which is proportional to the square root of the available fin torque.

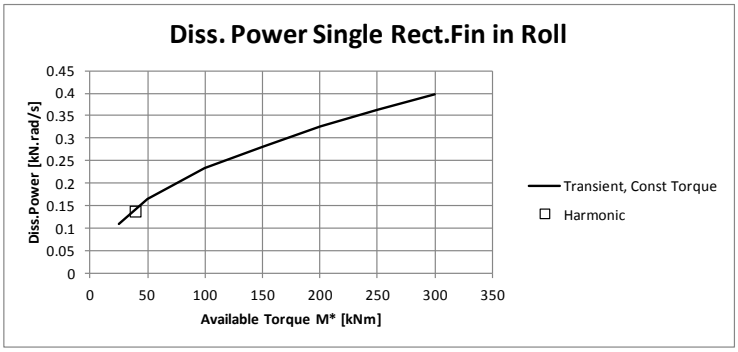

Figure 4 [*Damping power of a flapping fin as a function of the available actuator torque*]

5. 2008 EXPERIMENTS

The objective of the 2008 experiments was to explore the nature of the reaction forces and the related roll damping of flapping fins and to compare these with the conventional fin solution.

5.1 (a) Fin models

During the tests the fins (see Figure 5) were mounted on a flat plate. A digitally controlled servo engine on the back facilitated oscillations in a conventional rotation mode or a flapping mode.

Figure 5 [*Fin models*]

A rectangular fin with NACA0015 profile and a span of 175mm and a chord of 90mm was oscillated in a flapping mode; the set-up allowed an angular range up to 70deg. A limitation of the set-up was a rotation around a point 79mm below the base of the fin and a substantial gap between the base of the fin and the supporting plate.

The results were compared with measurements on a conventional NACA0015 fin with a span of 90mm and a mean chord of 175mm. The root gap of this fin was very small.

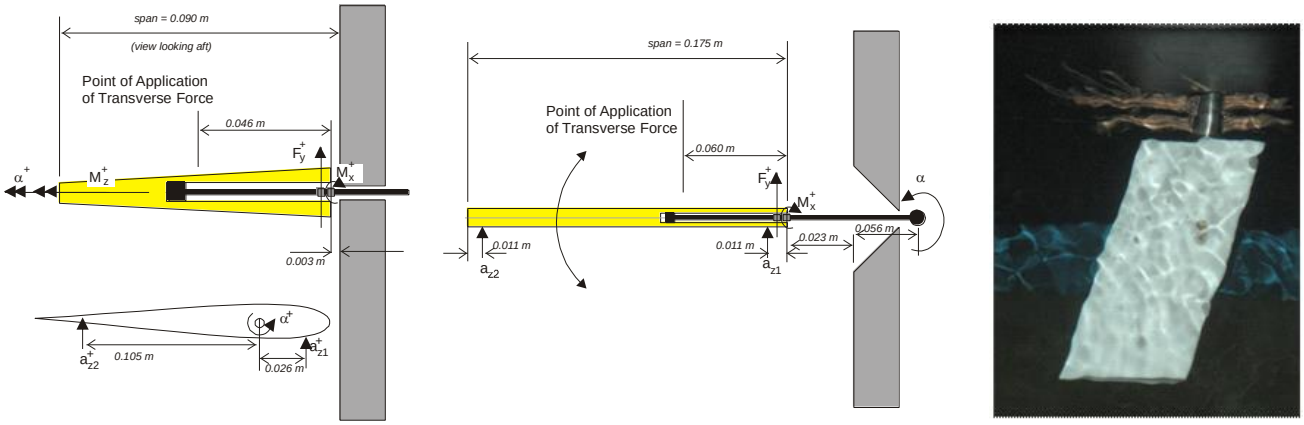

Figure 6 [*Fin test set-up*]

5.1 (b) Measurements

The measurements comprised 5 components of the reaction forces at the base of the fin body, linear accelerations at two points (to enable derivation of the angular acceleration) and the output angle of the servo unit.

5.1 (c) Fin actuator

At the time of the tests the kicking acceleration of the fin was regarded as a key parameter in the reaction forces. For this reason "hard kicking motions" were tested. This rather "aggressive" mode made us aware of the importance of a stiffness and the (the absence of) back-lash in the connections; vibrations of the fin on the transducer interfered with the hardware control loop inside the fin actuator servo. These vibrations made it hard to establish a clear relation between the fin motion and reaction forces. As shown by the most recent test results (see Section 6), new generations of servo units yield a better control over the actual maximum acceleration of the fin.

5.1 (d) Test programme

For the conventional fin the test programme comprised tests in a harmonic and "bang-bang" mode at zero and two non-zero speeds. In addition, the static lift and drag at forward speed were determined.
For the flapping fin, tests were performed in a bang-bang mode at zero and two non-zero forward speeds. The harmonic oscillation was only performed at non-zero speed.

For both types of fins the cycle time (corresponding to half the roll period of the ship to be stabilized), which equals the sum of the fin acceleration, the constant velocity and the deceleration and a "resting" period, was varied to obtain information about fluid-memory effects.

5.1 (e) Analysis

The measurements on the linear accelerations were used to derive the angular acceleration. The measured forces were corrected for the structural weight and inertia, which were derived from oscillation tests in air. The lift and drag, which were measured inside the rotating shaft, were corrected to obtain values in an earth-bound system of coordinates. These forces were correlated with the fin angular acceleration and velocity.

In addition to an analysis of the forces, the dissipated power of the reaction force in a virtual (1rad/s roll velocity) roll motion was evaluated. This quantity is the time averaged work performed by the linear reaction force in roll in Nrad/s. Derivation of the work of a pair of fins in roll requires multiplication by a factor of 2 (to account for a pair of fins) and the effective arm of the reaction force to the centre of gravity of the ship.

5.2 Results obtained for the flapping fin

5.2 (a) Nature of the reaction forces

Figure 7 illustrates the character of the signal measured on the flapping fin at zero speed (basic flapping fin, 2s cycle time, 70deg fin angle range, 150deg/s velocity). As indicated in the foregoing it shows that the acceleration and deceleration phases of the "kicking" motion vary quite erratically. Despite this behaviour the measured transverse force follows the measured acceleration quite well in these stages. In the intermediate stage, at constant velocity, the measurements suggest a more or less constant drag force.

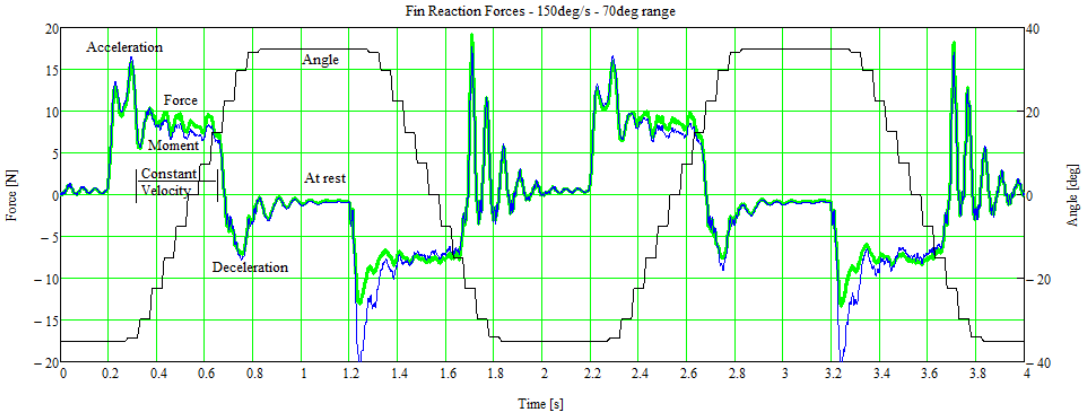

Figure 7 [*Reaction forces of flapping fin*]

The magnitude of the drag force is around 8.5N. The corresponding drag per unit velocity squared is $8.5/2.62^2=1.24N/(rad/s^2)$. Using the expression from Section 4.1, correcting for the fact that the rotation point is not at the base one obtains a force per unit angular velocity squared equal to $1/6.\rho.c_D.c.(s_{tip}^3-s_{base}^3)=0.245.c_D$. This suggests an effective drag coefficient of around 5 (which is typical for this kind of instationary flow; see also Section 6).

Calculating the point of application of the reaction force in the same way yields a point at 0.11m above the fin base; this is considerably larger than the value suggested by the fin force and moment measurements, which suggest an arm of 0.06m. It is concluded that the simple expression presented in Section 4.1 highly exaggerates the moment acting on the fin.

5.2 (b) Effect of forward speed, range, cycle time

Figure 8 summarizes the power dissipated by a single fin against a 1rad/s roll velocity. The results are given for the basic rectangular flapping fin in the bang-bang mode, for zero and two forward speeds and two fin angular velocities as a function of the angular minimum-maximum range.

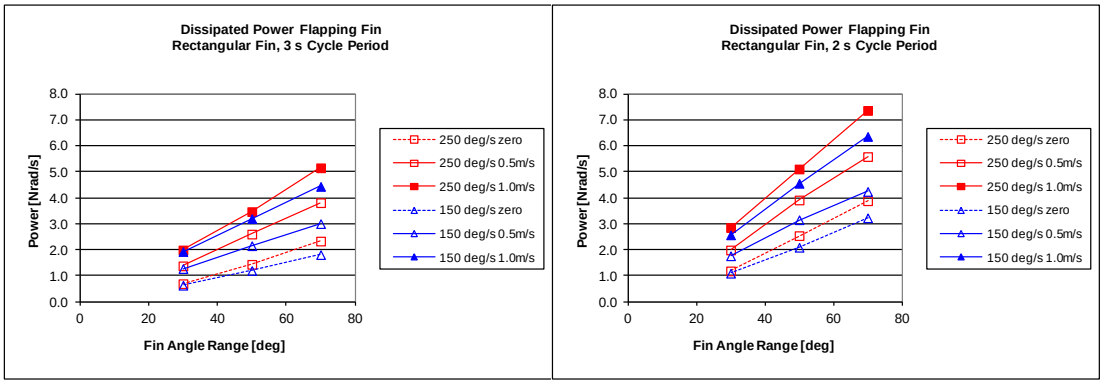

Figure 8 [*Effect of angular range on power dissipated in roll*]

The results can be understood by considering the nature of the reaction force discussed in the previous section. If we assume that the impulse contributions from the acceleration and deceleration stage largely cancel, the effective impulse of the reaction force follows from the force in the "stationary velocity" stage and the force, yielding 8.5 x 0.35s=3Ns. If the pulse is sufficiently short, the corresponding dissipated power[1] of two "kicks" over a full 2cycle roll period (per 1rad/s roll velocity) becomes 2 x 3/2=3Nrad/s. This value agrees well with the result of the analysis of the test results which considers the evolution of the roll velocity over the duration of the fin motion.

Effect of fin angle range
With an increasing fin angle range the reaction force does not always act in the ideal direction. In addition, the longer constant speed transit time decreases the work in roll. Despite these anticipated trends, the results in all conditions show that the work of the fin is proportional to the fin angle range.

Cycle time
A longer roll period associated with a longer cycle time reduces (also through an increase of the waiting time between "kicks") the work of the fin reaction force. It was expected that the cycle time would also affect the reaction forces through memory effects in the water. In practice these effects are limited.

Forward speed
At the lower fin velocity (150deg/s) the vertical velocity at the fin tip is about 2.62 x 0.254=0.66m/s. At 0.5m/s this implies a local angle of attack of over 50deg; at 1m/s forward speed this reduces to about 33deg. Despite the expected changes in the nature in the fin reaction forces (from "quadratic drag" to "linear lift") the magnitude increases very smoothly with increasing speed.

Figure 9 summarizes the foregoing trends with a plot of the product of the dissipated power and cycle time divided by the double-amplitude fin range and the square root of the fin velocity as a function of forward speed. These trends describe the over-all test results quite well. At 1m/s (a speed which correspond with some 8knots full scale for the present fin size) the fin reaction forces are roughly twice the values at zero speed.

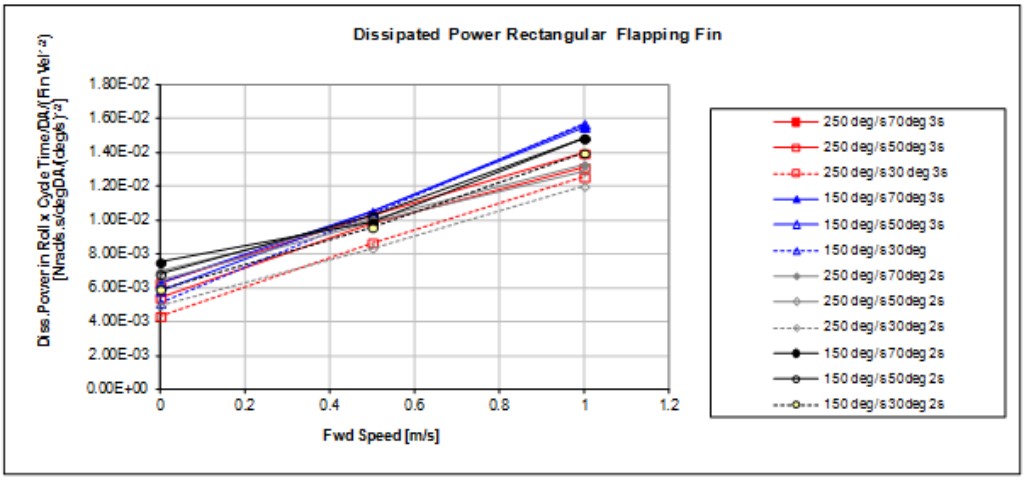

Figure 9 [*Dissipated power in roll x cycle time per deg fin angle range square root of the fin velocity*]

[1] Note that multiplication by the number of fins (often 2) and the arm to the CoG of the ship and an assumpition on the roll amplitude are required to obtain the roll damping. See sections 2.3 and 3.2.

5.3 Results obtained for the conventional fin

5.3 (a) Nature of the reaction forces

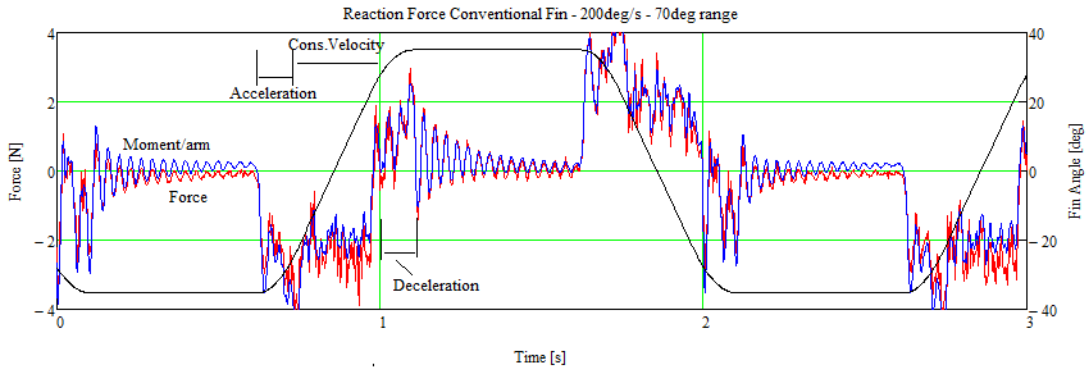

Figure 10: [*Reaction forces of conventional fin*]

The above figure shows a sample of the reaction force from a conventional fin at zero speed. As in the case of the flapping fin, the signals show considerable noise.

Despite the clear vibrations, the drag of the fin in the "constant velocity" stage can be recognized. The drag force, acting over a period of about 0.25s, amounts to about 2.5N, yielding an impulse of 0.625Ns. The related damping estimate amounts to 2 x 0.625 x 1rad/s/2s = 0.625Nrad/s.

The drag force amounts to $2.5/3.5^2 = 0.2N/(rad/s)^2$. The estimate from Section 4.1 yields $1/6.\rho.\pi.c_D.((c-a)^3-a^3)$, which amounts (with s=0.09, c=0.16 and a=0.033m) to $0.031.c_D$. This suggests an effective drag coefficient of 6.

The measured moment and force suggests a point of application at 0.075m aft of the shaft, a value which is somewhat smaller than that from the estimates on the moment and force from Section 4.1 (which yields 0.1m).

5.3 (b) Effect of forward speed, range and cycle time

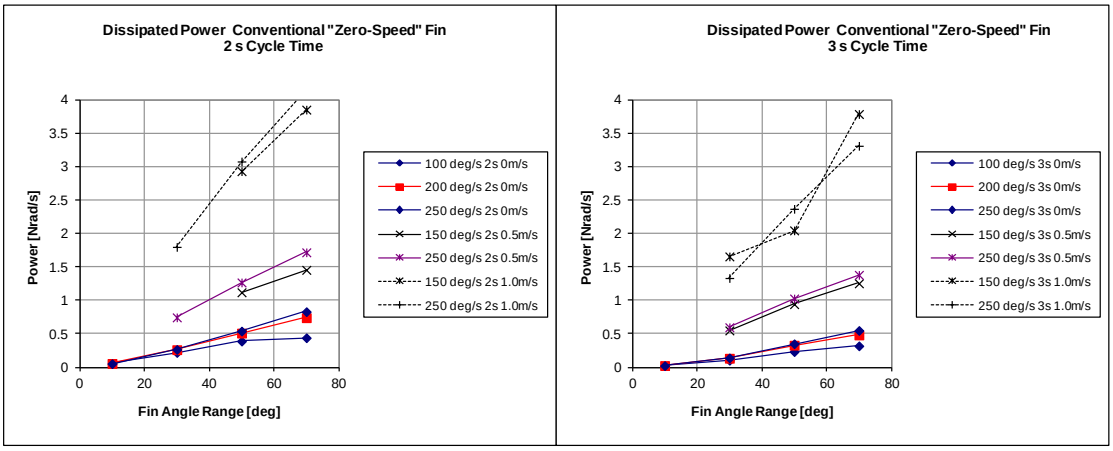

Figure 11: [*Dissipated power in roll of conventional fin*]

The figures above summarize the power dissipated by the conventional fin. The nature of the reaction force, being proportional to the fin angle range and decreasing with the cycle time, seems similar to the flapping fin; however the increase of the damping with forward speed seems much stronger.

5.3 (c) Comparison of a flapping and a conventional fin

The figure 12 shows results of a comparison of the work from both conventional and flapping fin systems at equal fin motions, velocities and accelerations.

Comparing the dissipated power in roll of both fins shows that the difference in performance is much larger than the small difference in fin area (the flapping fin was 9% larger than the conventional fin).

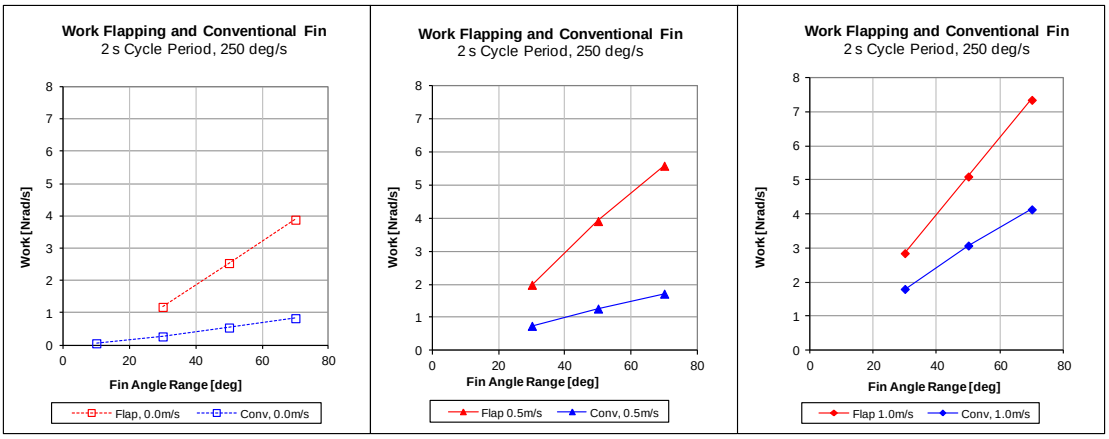

Figure 12: [*Comparison of dissipated work in roll of conventional and flapping fins*]

It is noted that, to achieve the same fin motions, velocities and accelerations, a flapping fin requires significantly more actuator power than a conventional fin. The comparison presented in Section 7 provided more information on this.

6. 2014 EXPERIMENTS

Perceiving advantages of flapping fins, AntiRoll BV developed an articulation which allows reduction of roll motion at both zero and forward speed. At zero speed, the fin is acting in a "flapping" mode while at forward speed it is acting in a conventional "rotating" mode. In addition, and if no active roll stabilisation is required, the AntiRoll fins can be retracted onto the hull.

Following extensive theoretical studies, and facing concrete applications, AntiRoll BV requested MARIN to perform an extensive test campaign which could be used as validation of the design tool. This was achieved through a two weeks test campaign in the MARIN Concept Basin (CB) in April 2014.

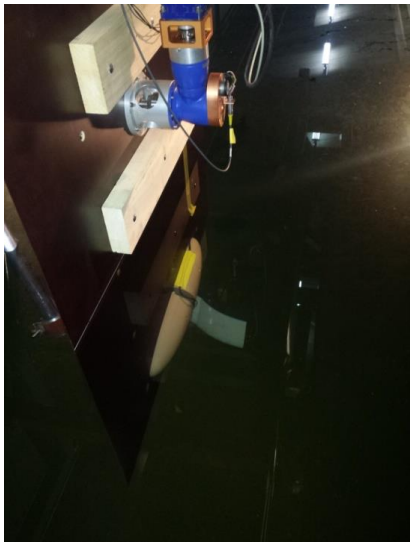

Figure 13 [*2014 test setup*]

6.1 General information

6.1 (a) Test setup

Contrary to the 2008 tests, the fin was mounted on a body of revolution, ensuring a minimal root-gap in the flapping mode. The set-up allowed activation of the fin in both flapping mode (used at zero and low forward speed) and rotative mode (used at forward speed).

Based on the experience gained with the test from 2008, a particular effort was made beforehand to ensure that the set-up was sufficiently rigid and the servo-control sufficiently fast to suppress vibrations.

6.1 (b) Fin models

Because the concept "parks" the fin along the hull when not in use, four different fin curvatures were tested. All 1:8 scale fins had an aspect ratio of 2, and a full scale area of 2 m^2. Each fin was fabricated out of injected PVC.

6.1 (c) Fin actuator

A powerful modern servo motor available at MARIN was used for this test. It was placed above the water level. The servo position and velocity were controlled via a feedback system.

6.1 (d) Test programme

For each fin the tests comprised:

- Four different flapping acceleration profiles at zero speed
- One harmonic flapping acceleration profile at several forward speeds
- Two harmonic rotating acceleration profiles at several forward speeds

6.1 (e) Analysis

Linear accelerometers were placed on the fin models and on the servo shaft to derive the angular acceleration. The measured forces were corrected for the structural weight and inertia, which were derived from oscillation tests in air. The lift and drag, which were measured inside the rotating shaft, were corrected to obtain values in an earth-bound system of coordinates. These forces were correlated with the fin angular acceleration and velocity.

In addition to the analysis of the forces, the power dissipated in a virtual roll motion by the fin reaction force was evaluated.

6.2 Results obtained for flapping fins at zero speed

The following results were obtained from a test with the straight fin model.

Figure 14 gives an impression of the quality of the set-up and measurements for a case with acceleration and deceleration transient phases of 120deg/s^2 and a maximum velocity of 65deg/s. The first three plots present the fin angle, angular velocity and angular acceleration. In these plots, the blue line represents the test measurement, while the red one represents the target values. From these figures, one may see that the target fin angle and the fin angular velocity were very well reproduced. Even the fin acceleration, which was harder to realize with the same accuracy, is rather well in line with the target value.

The lowest plot presents a comparison of the measured fin normal force and the estimated one. For the estimation of the force, a C_D of 5 was used. This comparison shows that the maximum peaks are not very well mimicked – possibly due to some residual variations in the test set-up – but the drag force and the global force shape are well estimated by the rather crude theoretical model detailed in Section 4.1 (a).

The present test campaign showed that the total required fin power and the realized damping in roll were estimated quite well by the theoretical model. Only the spanwise integration was truncated to allow for 3D "end effects".

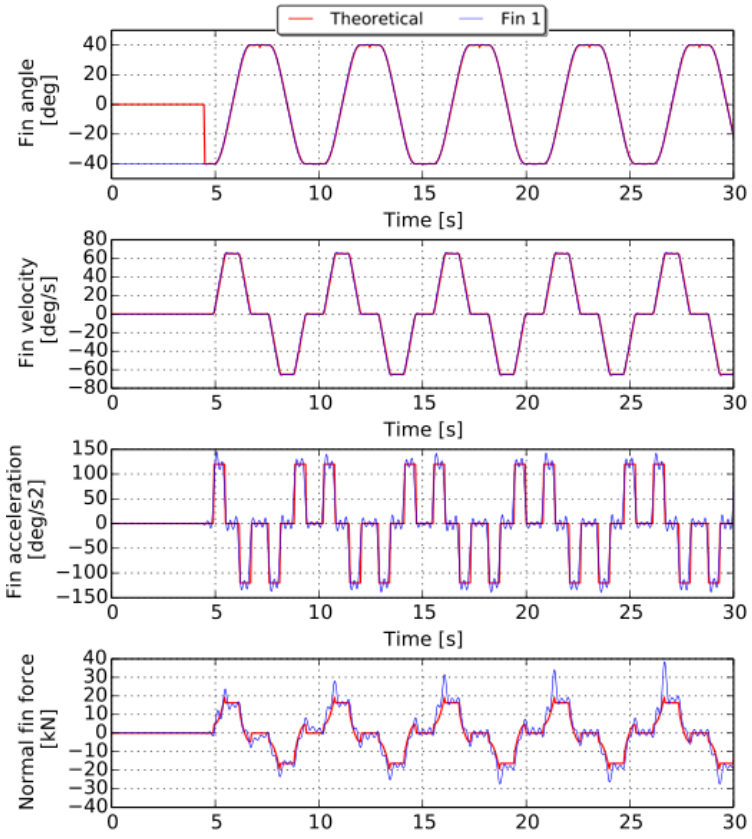

Figure 14 [*Measured and target fin angular motion, velocity, acceleration and normal force. The calculated normal force was obtained with a drag coefficient of 5*]

From the measured force and moment, the averaged point of application of the fin force is measured to be at 58% of the fin span. This result is rather well in line with the equations presented in Section 4, when taking into consideration the distance between the fin root and the fin pivot point.

6.3 Comparison of the rotating and flapping mode at forward speed

Fin damping
Tests at forward speed were performed with the fin in the flapping and rotating mode. Figure 15 compares the derived roll damping for harmonic fin motions for:

- A flapping mode with an angular range of +/- 40 degrees
- A rotating mode with an angular range of +/- 15 degrees

From this figure, it is seen that as expected, the fin damping obtained from rotating fins increases quadratically as a function of the forward speed while the damping obtained from flapping fins increases linearly above the zero-speed value. Up to rather high speeds – about 12kn – the flapping mode generates more damping than the rotating mode.

Of course, the power required to activate the flapping motions is much higher than that to activate the rotating motions.

Drag
The above tests showed (just as in 2008) that the false angles of attack in the flapping mode produce forward thrust at non-zero speed. In the conventional mode the fin yields an "induced" drag (see Hoerner, 1965) which is largely governed by the aspect ratio.

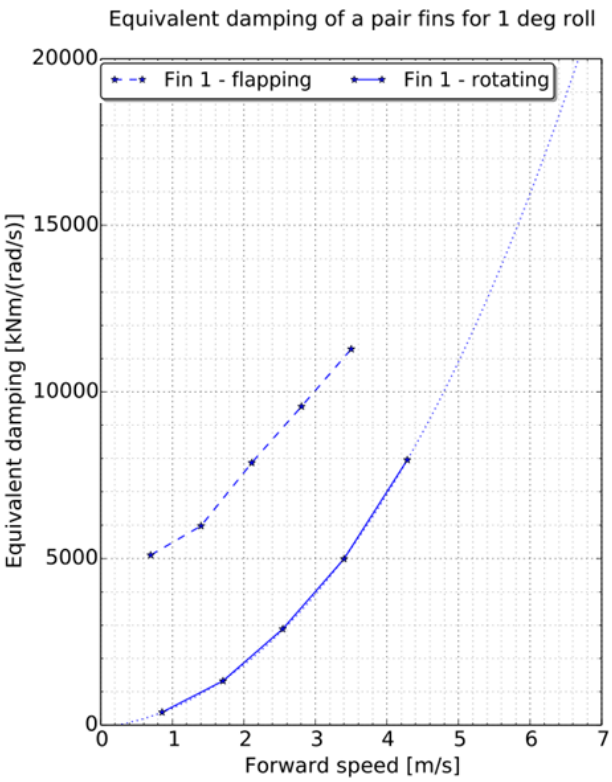

Figure 15 [*Roll damping from conventional rotating and flapping mode*]

7. MERITS OF FLAPPING FINS

Comparing flapping and conventional fins proved less straightforward than anticipated because the results depend on the details of the actuator limits and aspects of the fin arrangement. In the end we decided to make an assessment for a constant available actuator torque and a constant available instantaneous actuator power.

7.1 Basic fin forces

The assessment of the impulse and absorbed power of the fin reaction force builds on the expressions from Section 4.1 (truncating the integration to allow for end effects). Table 1 shows a comparison of a conventional fin and two flapping fins – one considering that the fin root is on the pivot point and one assuming that the fin root is at about 45% of the pivot point. This comparison assumes:

- Identical fin area
- The angular velocity and acceleration are only limited by the torque or the instantaneously absorbed actuator power
- The drag component dominates the impulse which yields the roll damping; the impulses from the initial acceleration and the deceleration are assumed to cancel each other

Regarding the results at constant torque the calculation shows that, while the reaction forces of the flapping fin are smaller than those of the conventional fin, the longer duration of the impulse yields a higher overall impulse. The increase over the conventional solution is at least some 20% (with the shaft at the fin base) and probably higher (the practicalities dictate a somewhat inboard location of the shaft).

At constant torque, as the travelled distance is the identical for all fins, the overall dissipated energy is the same. However, the flapping fin requires a lower instantaneous power.

Making the comparison at constant instantaneous power reduces the angular velocity of the conventional fin, leading to a substantial drop in the drag force. The resulting overall impulse of the flapping fin is at least some 40% higher. The total absorbed energy of the conventional fin is 25% lower.

	Designation		Conventional fin	Flapping fin	Flapping fin	units
	Conventional fin	Flapping fin	shaft at 20% of the chord	Fin root at the shaft	Fin root at 45% of the span from shaft	
Fin descriptions	Chord leading edge wrt shaft	Span root wrt shaft	-0.03	0.00	0.08	m
	Chord trailing edge wrt shaft	Span tip wrt shaft	0.14	0.18	0.25	m
	Span	Chord	0.09	0.09	0.09	m
	Aspect ratio		0.51	1.94	1.94	-
	Drag coefficient		5.00	5.00	5.00	-
	Drag force / α_v^2		0.22	0.41	1.22	N/(rad/s^2)
	Drag moment / α_v^2		0.02	0.05	0.24	Nm/(rad/s)^2
	Angular range		60.00	60.00	60.00	deg
Given an actuator torque	**Actuator torque**		**1.00**	**1.00**	**1.00**	**Nm**
	Resulting angular velocity		374.76	246.39	117.51	deg/s
	Duration of constant speed phase (Δt)		0.16	0.24	0.51	s
	Drag force		9.54	7.62	5.14	N
	Impulse: Drag Force . Δt		1.53	1.86	2.62	N.s
	Instantaneous actuator power		6.54	4.30	2.05	W
	Absorbed actuator energy		1.05	1.05	1.05	Ws
Given an actuator power	Actuator torque		0.72	0.95	1.56	Nm
	Resulting angular velocity		318.10	240.52	146.82	deg/s
	Duration of constant speed phase (Δt)		0.19	0.25	0.41	s
	Drag force		6.87	7.26	8.02	N
	Impulse: Drag Force . Δt		1.30	1.81	3.28	N.s
	Actuator power		**4.00**	**4.00**	**4.00**	**W**
	Absorbed actuator energy		0.75	1.00	1.63	Ws

Table 1 [*Comparison of a conventional and a flapping fin*]

7.2 Additional considerations

An additional aspect of the comparison is the fact that the point of application of the reaction force of a flapping fin is at a larger distance from the CoG. For a typical configuration we expect an increase of some 10% on top of the foregoing.

In addition to the above there are differences which are harder to quantify. We imagine the following:

- Flapping fins are not necessarily in line with bilge keels, allowing longer and higher bilge keels without negative interaction effects
- The limited chord at the root and the smaller angular motions of a high-aspect ratio fins limit the loss of lift in the rotating mode due to the root gap and significantly reduce the fin lift-induced drag (up to 75%).
- Conventional fins are less susceptible to a sudden loss of performance due to stall
- In case the perceived advantages materialize in smaller dimensions, flapping fins may yield a lower overall drag penalty.

8. CONCLUSIONS

Considering the results of the 2008 and 2014 test campaigns and the results of the simplified calculation method, it seems justified to conclude that:

- The modelling and measuring of transient motions of flapping fins is not entirely straightforward. The results of the 2014 campaign showed a much clearer relation between the fin motions and reaction forces.
- With some adaptations the theoretical model developed for zero speed stabiliser fins reproduces the test results fairly well.
- The damping from zero speed fins is largely governed by the angular velocity, the angular range, the cycle time and forward speed.
- Depending on the details of the actuator and the fin arrangement, a flapping fin seems to offer clear advantages in the lower speed range.

Follow-up
Recognizing the complexity of the flow around flapping and stalling fins, MARIN has initiated a 2-year post-doc investigation to obtain an understanding of the physics of dynamic stall by means of CFD.

9. ACKNOWLEDGEMENTS

The authors gratefully acknowledge the permission of AntiRoll BV for using part of results from the 2014 test campaign.

10. REFERENCES

Dallinga, R.P., "Roll stabilization of motor yachts: Use of fin stabilizers in anchored conditions", *Project 1999 Symposium,* Amsterdam, 1999

Dallinga, R.P., "Hydromechanic aspects of the design of fin stabilizers", *RINA Spring Meeting,* London, 1993

Dallinga, R.P., "Roll stabilization at anchor: Hydrodynamic aspects of the comparison of anti-roll tanks and fins", *Project 2002 Symposium,* Amsterdam 2002

Gaillarde, G., "Dynamic stall and cavitation of stabilizer fins and their influence on the ship behaviour", *FAST,* Napels, 2003

Hoerner, S.F, "Fluid – dynamic drag, theoretical, experimental and statistical information", 1965

Licht, S., Hover, F. and Triantfyllou, M.S., "Design of a flapping foil underwater vehicle", *Int. Symp. on Underwater Technology,* 2004.

Oossanen, P.van, "A method for the calculation of resistance and sail force of sailing yachts", *RINA Conf. on Calculator and computer aided design for small craft – The way ahead,* Southampton, 1981

Soueid, H., Propulsion by mobile wings: Aerodynamic and applications to micro air vehicles, *DIAM, University di Genova, Internal Report 02,* 2005